Chemical Engineering Journal, Volume 372, 15 September 2019, pp. 886-895
DOI: 10.1016/j.cej.2019.04.080

Structural and kinetic analysis of CO_2 sorption on $NaNO_2$-promoted MgO at moderate temperatures

Ke Wang[1,2], Youwei Zhao[1], Peter T. Clough[2], Pengfei Zhao[1], Edward J. Anthony[2*]

[1] School of Electrical and Power Engineering, China University of Mining and Technology, Xuzhou 221116, China.

[2] Energy and Power Theme, Cranfield University, Cranfield, Bedfordshire, MK43 0AL, UK.

Ke Wang is currently visiting Cranfield University.

* Corresponding author: Edward J. Anthony, E: b.j.anthony@cranfield.ac.uk, T: +44 (0) 1234 752 823

Abstract: Alkali metal nitrate-/nitrite-promoted MgO sorbents are promising candidates for intermediate-temperature (200-500 °C) CO_2 capture. However, the structure-performance relationship and kinetic characteristics of $NaNO_2$-promoted MgO remain unclear. Here the effects of physical-chemical properties on the CO_2 sorption performance of $NaNO_2$-promoted MgO and the sorption kinetics were comprehensively studied to elucidate the detailed role of $NaNO_2$. Samples were characterized by X-ray diffraction, scanning electron microscopy, N_2 adsorption, Fourier transform infrared spectroscopy and X-ray photoelectron spectroscopy. The sorption kinetics were obtained by isothermal thermogravimetry and elucidated using a double exponential model. Compared with pure MgO and $NaNO_3$-promoted MgO, $NaNO_2$-modified MgO had a lower initial sorption temperature and a unique bimodal sorption characteristic. Characterizations results revealed that such bimodal sorption

was due to the presence of double promoters (mixture of $NaNO_2$ and $NaNO_3$) which implies that some of the nitrite was oxidized to nitrate during the preparation process. Deposition of double promoters further reduced the amounts of hydroxide and carbonate species for pure MgO while still preserving more hydroxide and carbonate species on the surface as compared with $NaNO_3$-promoted MgO. The kinetics analysis demonstrated that the double exponential model can well-describe the sorption process for both $NaNO_3$- and $NaNO_2$-promoted MgO, suggesting that the entire sorption occurs as a double process (surface chemisorption and product layer diffusion). Significantly differences were seen from $NaNO_3$-promoted MgO, and the surface chemisorption process of $NaNO_2$-promoted MgO was independent of temperature, which suggests that an increased presence of hydroxide and carbonate species provide more active sites for greatly facilitating surface chemisorption.

Keywords: CO_2 capture; $NaNO_2$; $NaNO_3$; MgO

1. Introduction

The current CO_2 concentration in the atmosphere is the major contributor to climate change [1]. According to the International Energy Agency (IEA) report, the global CO_2 emissions from fossil fuel combustion have risen to over 30 Gt/year [2]. While new carbon-free energy sources are being developed, fossil fuels will remain an indispensable source of energy in the near future, particularly in developing countries [3]. For this reason, CO_2 capture and storage (CCS) is currently the most attractive solution to avoid drastic climate change [4].

Oxy-combustion [5, 6], post-combustion [7, 8] and pre-combustion [9, 10] are three major advanced CO_2 capture technologies for coal power plants. More recently, calcium-based materials and ceramic sorbents which have high-capacity CO_2 uptake at elevated temperatures (>400 °C), are also being explored [11]. However, in pre-combustion capture systems (gasification or natural gas reforming), solid sorbents at intermediate temperatures (250-400 °C) offer a lower energy penalty than low-temperature aqueous amines, as they avoid the process of cooling and reheating the regeneration step [12]. Moreover, *in situ* CO_2 uptake can produce high-purity hydrogen during the sorption-enhanced water gas shift process [9]. Hydrotalcite-like anionic clays have also been proposed for CO_2 removal through surface sorption at intermediate temperatures in the 300–400 °C range. However, hydrotalcites offer relatively low CO_2 uptake capacities [13, 14]. Recently, MgO has been recognized as a promising intermediate-temperatures candidate, based on its unique features: (i) MgO possesses moderate basicity, which can capture the acidic CO_2 and it offers a high theoretical capture capacity of 1.09 g CO_2/g MgO; (ii) as compared to other possible basic metal oxides (CaO and Li_4SiO_4), MgO requires a relatively low regeneration temperature (~500 °C), thus consuming less energy for its regeneration; and (iii) MgO-based materials are noncorrosive, nontoxic, abundant in nature and available at a relatively low cost [15, 16] .

Unfortunately, the CO_2 capture properties of most MgO-based sorbents is far from satisfactory, due to their relatively weak sorption kinetics, low sorption capacity and poor stability. For instance, commercial MgO powder exhibits an extremely low

capacity (0.02 g CO_2/g MgO) at 200 °C mainly due to its slow kinetic reactivity. To improve its reactivity, obtaining MgO with smaller particle size [17], using porous MgO and incorporating MgO into porous supports have all been proposed [18, 19]. However, these modified MgO particles with increased specific surface area have achieved only limited success [20]. Increasing the pressure may increase the reaction rate, but this is problematic for practical applications [21]. Alternatively, the use of steam can improve the CO_2 sorption rates of MgO due to the formation of $Mg(OH)_2$, [22]. Nevertheless, the practical temperature range for this sorbent is limited to 200-315 °C.

Fortunately, doping alkali salts into MgO can significantly facilitate the sorption of CO_2 [20]. These alkali salts can be classified into four categories, i.e., single components [23-27], double salts [28-31], triple salts [32-35] and multiple salts [36, 37]. For K_2CO_3-doped sorbents, recent studies indicate that the CO_2 sorption ability was increased to 10.2-11.7 wt% [38, 39]. Na_2CO_3 and $NaNO_3$ co-doped MgO presented higher capacity (15 wt%), which was mainly attributed to the formation of the sodium-magnesium double carbonate ($Na_2Mg(CO_3)_2$) and the additional promoting effect of $NaNO_3$ [29]. Alkali nitrate-promoted MgO [40, 41], especially $NaNO_3$-MgO also demonstrated relatively fast CO_2 sorption rates, with the sorption capacity reaching ~60 wt% in 120 min [24, 41]. Recently, multiple $NaNO_2$-based promoters ($NaNO_3$-$NaNO_2$ and $LiNO_3$−(Na−K)NO_2) have been incorporated into mesoporous MgO or colloidal nanoclusters of MgO to improve capture. In general, the addition of such multiple $NaNO_2$-based salts further enhanced both the kinetics

and the CO_2 sorption capacity of $NaNO_3$-modified MgO [31, 32]. To date, previous studies on developing $NaNO_2$-modified MgO have three shortcomings. (1) The CO_2 uptake performance dependence on the appropriate temperature range has not been comprehensively examined. (2) It has been reported that the formed MgO-NO_x species have high concentrations of oxide ions (O^{2-}) and allow the fast generation of carbonate ions (CO_3^{2-}), in turn, enabling rapid nucleation and growth of $MgCO_3$ crystals [31, 32]. However, the types of active sites present on the surface of MgO have not been clearly identified. (3) A suitable kinetic model for the CO_2 sorption process by $NaNO_2$-coated MgO is not available. Furthermore, there is only one study on the kinetics of $NaNO_3$-$NaNO_2$-promoted MgO, which is limited as it was carried out at a fixed temperature [31]. Here, to elucidate the detailed role of $NaNO_2$ in a promoting system, dynamic and isothermal thermogravimetric analyses were conducted to obtain CO_2 uptakes performance dependence on different temperature ranges. The effects of physical-chemical properties of the sorbents on the CO_2 sorption performance are also explored by means of a detailed structural characterization to identify the types of active sites on the surface of MgO. Moreover, a double exponential model combined with detailed temperature dependence mapping of the sorption process in a specific temperature range have been developed.

2. Experimental

2.1. Sorbents

The magnesium carbonate hydroxide hydrate ($4MgCO_3 \cdot Mg(OH)_2 \cdot xH_2O$), $NaNO_3$, and $NaNO_2$ used in this study were analytical grade and supplied by

Shanghai Aladdin Reagent Co., China.

In the preparation procedure, pure MgO was first obtained by calcining magnesium carbonate hydroxide hydrate in a muffle furnace at 450 °C for 3 h with a heating rate of 3 °C/min. Then, sodium nitrite was added with a mass ratio of $NaNO_2$:MgO of X:1 (X = 0.1, 0.15, and 0.2); after fully mixing, the powder was calcined again in a muffle furnace at 450 °C for 3 h. The resulting samples were collected and are labeled as MgO/X$NaNO_2$. For comparison, the sodium nitrate-promoted MgO sorbent (labeled as MgO/0.2$NaNO_3$) was also synthesized by the above procedure but only with a mass ratio of 20% $NaNO_3$ addition.

2.1.1 Characterization

The phase composition and crystallographic structure of each sample were examined by powder X-ray diffractometry (XRD: Rigaku D/max 2550 X-ray diffractometer). The operating parameters were Cu Kα target (λ = 0.154 nm) and 40 kV/100 mA power generator. A scan range of 10-80° (2θ) was measured with a step size of 0.02° and a speed of 0.1 sec/step. The size and morphology of the sorbents were characterized via scanning electron microscope (SEM: JSM-6360LV). The Fourier transform infrared (FTIR) spectra were recorded using a Bruker (Germany) Vertex 80v spectrometer. The spectra were collected in the wave length region of 4000-400 cm^{-1}, and 32 scans were accumulated at 4 cm^{-1} resolution. The chemical valence states on the surface were analyzed using X-ray photoelectron spectroscopy (XPS: Perkin-Elmer, PHI 5600). The specific surface area (BET) and desorption average pore diameter (BJH) analyses were conducted with a NOVA 2000

Quantachrome instrument.

2.1.2 Sorbent performance tests

A ZRY-1P thermogravimetric analyzer (TGA) (Techcomp Jingke Scientific Instrument Co., Ltd., Shanghai, China) was used to analyze the CO_2 sorption properties of the sorbents. Approximately 10 mg of the sample was placed in a crucible and heated from 100 °C to 600 °C at a rate of 7 °C/min under a pure CO_2 flow of 50 mL/min. For this work, the isothermal sorption properties were tested as follows. The samples were heated to a specific temperature (240, 260, 280, 300, 320 or 340 °C) under N_2 atmosphere (50 mL/min), then the flow gas was immediately switched to pure CO_2 (50 mL/min), and the sample maintained at the specific temperature for 180 min. In order to evaluate the cyclic sorption properties, 10 sorption/desorption cycles were examined as follows: CO_2 sorption was performed at 300°C (for MgO/0.2$NaNO_3$) or 320 °C (for MgO/0.2$NaNO_2$) in pure CO_2 (50 mL/min) for 60 min, and desorption was performed at 400 °C in pure N_2 (50 mL/min) for 10 min.

3. Results and Discussion

3.1 CO_2 uptake performance

Fig. 1 summarizes the CO_2 uptake performance of MgO sorbents coated with alkali nitrates/nitrites in 100% CO_2 atmosphere. The MgO sorbents with alkali nitrates/nitrites were explored over a wide temperature range (from 100 °C to 600 °C), as shown in Fig. 1a. The pure MgO sample presented very low CO_2 sorption performance (maximal uptake of 0.02 g/g), and is not shown here. When coated with

20 wt% $NaNO_3$, $MgO/0.2NaNO_3$ began to gain weight at around 250 °C and reached a maximal weight increase of 0.54 g/g at ~380 °C. The initial sorption temperature (250°C) is below the melting point of $NaNO_3$ (308 °C). Thus, this behavior is associated with the "pre-molten" phenomenon, which produces a metastable liquid film at solid interfaces even prior to reaching the melting temperature [42, 43]. However, beyond 400 °C, the sorbent started to release CO_2 (weight decrease). Furthermore, compared with pure MgO, the CO_2 uptake was markedly improved for $MgO/0.2NaNO_3$ and $MgO/0.2NaNO_2$. In particular, in comparison with $MgO/0.2NaNO_3$, three important features can be observed for the case of the 20-wt% $NaNO_2$ coating. First, its initial sorption temperature was lower, as it began to sorb CO_2 as early as 220 °C. Second, its CO_2 uptake process presented specific variations as shown in Fig. 1b (DTG, derivative thermogravimetry curve). For $MgO/0.2NaNO_3$, there was only one strong peak at ~280 °C, where the maximal CO_2 sorption rate occurs. However, two peaks were observed for the case of $MgO/0.2NaNO_2$, one at ~268 °C and the other at ~305 °C. This bimodal sorption characteristic of $MgO/0.2NaNO_2$ was further observed in the DTG curves of $NaNO_2$ and $NaNO_3$ co-doped MgO (molar ratio of $NaNO_2$ to $NaNO_3$ at 0.09:0.11) as shown in the Supporting Information (Fig. S1a). However, the phenomenon of two peaks did not appear for $NaNO_3$-coated MgO or $NaNO_3$ and Na_2CO_3 co-doped MgO as shown in Fig. S1b-c. The results above confirm that the presence of $NaNO_2$ is required to produce the bimodal sorption characteristic. The unique sorption characteristic of $MgO/0.2NaNO_2$ may result from the presence of double promoters (mixture of

$NaNO_2$ and $NaNO_3$) since the melting points of $NaNO_2$ (271 °C) and $NaNO_3$ (308 °C) agree with the temperature for both peaks in the DTG curves. Finally, its reaction rate and the maximal sorption capacity were both significantly enhanced. The CO_2 uptake process of MgO/0.2$NaNO_2$ presented a significantly greater weight increase compared with MgO/0.2$NaNO_3$. Here, the maximal weight increase of MgO/0.2$NaNO_2$ was 0.62 g/g, higher than the case of MgO/0.2$NaNO_3$ (0.54 g/g). This superior performance demonstrates that $NaNO_2$ serves as a more effective promoter than $NaNO_3$.

To further determine the optimal proportion of $NaNO_2$, three dynamic sorption tests of MgO sorbents coated with $NaNO_2$ in different proportions were carried out, as shown in Fig. 1. When the proportion was less than 20 wt% (i.e., 15 wt%), the sorption rate of CO_2 was slower and the maximal sorption capacity reached only 0.53 g/g. As the amount of $NaNO_2$ was increased above 20 wt% (i.e., 25 wt%), the sorption rate between 200 and 260 °C was slightly faster, while the maximal uptake capacity dropped significantly to a value of 0.49 g/g. These observations are similar for the case of $NaNO_3$-promoted MgO reported in previous work [26, 41]. With an increase of the amount of $NaNO_2$, the CO_2 uptake capacity began to decrease beyond a critical point, which was attributed to the weakened triple-phase boundaries (TPB) [26]. Here, the optimal proportion of $NaNO_2$ is 20 wt%. In addition, all $NaNO_2$-promoted samples presented bimodal sorption behavior (Fig. 1b), which again highlighted its double promotion effect.

According to the dynamic tests, the promotion effect generated by nitrate/nitrite

addition was observed primarily between 240 °C and 340 °C. Thus, Fig. 2 compares the isothermal sorption curves of $MgO/0.2NaNO_3$ and $MgO/0.2NaNO_2$ at 240, 260, 280, 300, 320 and 340 °C. The isotherm of uncoated MgO was also provided for comparison. Uncoated MgO achieved an extremely low CO_2 uptake of 0.012 g/g within a few minutes and maintained that value throughout the subsequent process. CO_2 uptake for the two promoted samples was much higher, as shown in Fig. 2a-b, with the total uptake of ~0.53 and 0.61 g/g for $MgO/0.2NaNO_3$ and $MgO/0.2NaNO_2$, respectively.

Compared with the pure MgO, the isothermal sorption curves of the two promoted samples display a three-step sorption process, proceeding through an initial induction step and a second fast surface chemisorption step followed by a third relatively slow diffusion step. As shown in Fig. 2c, during the initial induction step, there is a time period (~4 min) required to initiate the sorption of CO_2 for $MgO/0.2NaNO_3$, which we attribute to the formation of carbonate species on the partially active sites on the surface of MgO [26, 33].

It is also clear that the sorption rate and capacity depend on not only the temperature but also the type of promoters. At low temperatures (240-260 °C), the $MgO/0.2NaNO_3$ exhibited relatively low CO_2 uptake, reaching less than 35 wt% after 3 h. By comparison, $MgO/0.2NaNO_2$ demonstrated faster weight increases, which indicates that the formed $MgCO_3$ product layer of $MgO/0.2NaNO_2$ is thicker than that of $MgO/0.2NaNO_3$. Such thicker product layers may have greater resistance for CO_2 diffusion. Thus, it trapped less CO_2 after 180 min (30 wt%) than $MgO/0.2NaNO_3$.

Further increasing the temperature to 280-300 °C, CO_2 sorption for two sorbents was significantly enhanced as the diffusion process was activated. At 300 °C, the uptake for MgO/0.2$NaNO_3$ was nearly saturated at ~55 wt% by 120 min. MgO/0.2$NaNO_2$ presented a similar but even better enhanced behavior as it became quickly saturated at ~55 wt% within 60 min. Fast kinetics are especially desirable for practical applications since the *in situ* CO_2 uptake should be quick enough, for example, to produce high-purity hydrogen during the sorption-enhanced water gas shift process [9]. Interestingly, the saturated sorption capacities of both samples were nearly identical after an extended reaction time (180 min). However, as the temperature was increased to 320-340 °C, some changes occurred in the CO_2 sorption process. Their sorption rates decreased during the initial period whereas the final uptakes were slightly improved. This observation was mainly due to the increased CO_2 equilibrium concentration in the molten salts and the enhanced diffusivity of CO_2 in the product layer with increasing temperature.

In addition, when the sorption temperature was higher than 300 °C (i.e., 320 °C), a sharply depressed sorption rate was obtained for MgO/0.2$NaNO_3$, suggesting that its optimal temperature is 300 °C. The optimal temperature for MgO/0.2$NaNO_2$, on the other hand, shifted higher (320 °C), and a relatively higher uptake and faster sorption rate were observed at 320 °C. Moreover, MgO/0.2$NaNO_2$ exhibited a faster sorption rate and higher uptake capacity over a wider temperature range, which is convenient for practical applications such as gasification or natural gas reforming [9].

3.2 Structural characterization

To explain the higher CO_2 capture performance of MgO/0.2$NaNO_2$, XRD, SEM, N_2 adsorption, FTIR and XPS analyses were performed. Fig. 3 shows the XRD patterns of different MgO-based samples. The diffraction pattern of pure MgO sample presented the typical cubic phase of MgO (JCPDS files 75-0447). The crystallite size of pure MgO estimated by the Scherrer's equation was determined to be 8.0 nm as listed in Table 1. After the coating treatment, clear diffraction peaks of $NaNO_3$ were identified in MgO/0.2$NaNO_3$, and both $NaNO_2$ and $NaNO_3$ were observed in MgO/0.2$NaNO_2$, which shows that some of the nitrite appears to be oxidized to nitrate during the preparation process. Moreover, compared with the pure MgO sample, the MgO diffraction peaks of the two coated samples both became sharper with higher intensity. As shown in Table 1, when coated with $NaNO_3$ and $NaNO_2$, the crystallite size of MgO increased up to 14.3 nm and 13.7 nm, respectively. Such an increase in the crystallite size of MgO was also observed in other alkali-salt-coated MgO sorbents. This may be attributed to the shrinkage of the composite due to the low melting temperatures of $NaNO_3$ and $NaNO_2$ during the calcination process.

The morphologies of three MgO samples were further examined by SEM images. In Fig. 4a, uncoated MgO generally displayed an ellipsoidal structure. This similar morphology was also observed in MgO/0.2$NaNO_3$ and MgO/0.2$NaNO_2$ at this resolution (Fig. S2). However, differences are observed at higher resolution. Uncoated MgO presented a smooth sheet-like structure (Fig. 4b). When coated with $NaNO_3$, MgO also exhibited a sheet-like structure (Fig. 4c); however, its surface became rather rough, indicating that $NaNO_3$ covered the surface of MgO. The fuzzier

morphology of $NaNO_2$-coated MgO is further shown in Fig. 4d. It can be seen that MgO/0.2$NaNO_2$ still preserves the sheet-like structure while its surface is rougher. Due to its lower melting point, $NaNO_2$ had a greater tendency to sinter, facilitating its coating on the MgO surface during the calcination process.

The XRD and SEM results were further confirmed by N_2 adsorption analysis. As shown in Fig. 5a, all adsorption-desorption isotherms exhibited the characteristics of type-IV isotherm and type-H3 hysteresis loop, indicating a typical mesoporous structure. Their pore size distributions, as shown in Fig. 5b, were all mainly centered at ~3 nm, suggesting their high mesoporosity. When coated with the nitrate/nitrite salts, the specific surface area given in Table 1 and pore volume shown in Fig. 5b dropped dramatically, indicating that large amounts of mesopores were filled by molten nitrate/nitrite during the calcination process. In particular, MgO/0.2$NaNO_2$ displayed the lowest specific surface area and pore volume, which is unsurprising given its highly sintered morphology and the larger MgO crystallite size. The change in phase composition, morphology and textural properties after coating with $NaNO_3$/$NaNO_2$, indicate that these alkali metal nitrates/nitrites were incorporated into the MgO. Moreover, with regard to their CO_2 uptake performance, it was noted that the CO_2 uptake of the three MgO sorbents are not directly proportional to their surface areas and pore volumes (as shown in Table 1). These observations agree with previous studies [26, 41], suggesting that the presence of alkali nitrates or nitrites is more important than the resultant morphology for their CO_2 sorption processes.

FTIR and XPS were further conducted to identify the active sites on the surface

of MgO. Fig. 6 shows the variations in the FTIR spectra of samples before sorption (Fig. 6a) and after sorption (Fig. 6b). As shown in Fig. 6a, for pure MgO, peaks ascribed to O-H stretching vibrations for various types of hydroxyl groups at 3727, 3625 and 3486 cm^{-1} were identified, suggesting that the oxygen sites on the surface of MgO were partially protonated [44]. A broad peak at ~1500 cm^{-1} and a shoulder at 1630 cm^{-1} attributed to asymmetric stretching of unidentate/bidentate carbonates were also evident, implying that the adsorption of atmospheric CO_2 occurs on the surface of MgO [45]. Following coating with $NaNO_3$, a sharp peak attributed to N−O stretching vibration for nitrate (NO_3^-) groups was observed at 1384 cm^{-1} [34]. For the case of MgO coated with $NaNO_2$, beside N−O stretching vibration for NO_3^- groups, one additional shoulder corresponding to N−O stretching vibration for nitrite ion (NO_2^-) groups was also observed, at 1269 cm^{-1} [32]. The appearance of both NO_3^- and NO_2^- is in accord with the XRD analysis, indicating that some of the nitrite in MgO/0.2$NaNO_2$ has been oxidized to nitrate. After the coating treatment, the asymmetric stretching of unidentates (at ~1500 cm^{-1}) disappeared and was replaced by N−O stretching vibration for NO_3^- and NO_2^- (at 1384 and 1269 cm^-) [34]. These changes indicate that most atmospheric CO_2 adsorbed on MgO decomposed during the coating process and new nitrates/nitrites (NO_x^-) were generated that coordinated chemically on the MgO surface. Furthermore, the peaks corresponding to O-H stretching vibrations for various types of hydroxyl groups changed for the coated MgO particles. Interestingly, both peaks corresponding to O-H stretching vibrations for various types of hydroxyl groups and N−O stretching vibration in MgO/0.2$NaNO_2$

are stronger than those for MgO/0.2$NaNO_3$. For comparison, we normalized all spectra of two sorbents by the absorbance at 1384 cm^- (NO_3^-). As shown in Fig. S3, larger amounts of hydroxide sites on the surface of MgO were preserved in MgO/0.2$NaNO_2$ as its peaks corresponding to O-H stretching vibrations were stronger than for MgO/0.2$NaNO_3$.

Fig. 7 depicts the X-ray photoelectron spectra orbitals for the three MgO samples before sorption and two samples after sorption. For fresh MgO/0.2$NaNO_3$, the main peaks assigned to $NaNO_3$ were identified at 407.3 ev and 1071.6 ev in the survey scanned region of the N 1s and Na 1s spectra (Fig. 7a), respectively, supporting the hypothesis that NO_3^- species are located on the MgO surface. Compared with the case of MgO/0.2$NaNO_3$, a slight shift was observed in the high-resolution spectrum of Na 1s for MgO/0.2$NaNO_2$ (Fig. 7b), which is probably due to the presence of $NaNO_2$ [46]. Furthermore, the high-resolution spectrum of O 1s for pure MgO shows two main peaks at ~528.5 and 531.8 ev (Fig. 7c), which indicate the presence of hydroxide and carbonate species, respectively [47]. In line with the FTIR results, XPS analysis suggested that there are two types of active sites on the surface of MgO, the former representing hydroxyl groups and the latter arising from atmospheric CO_2 adsorption on the surface of MgO. After the coating treatment, the intensity of carbonate species was decreased markedly, implying that most of the atmospheric CO_2 adsorbed on MgO was replaced by NO_x^-, whereas, the hydroxide sites on the surface of MgO have been preserved, especially for MgO/0.2$NaNO_2$, since its intensity is almost comparable to the case of pure MgO, as shown in Fig. 7c. Moreover, accompanied

with the change of their binding energies, a slight shift of O 1s peaks toward the lower binding energies was observed in the spectra of both coated samples, corresponding to the presence of NO_x^- species with their larger binding energies (~532.6 ev) [46]. Such change indicated that the coated nitrate/nitrite salts react with MgO chemically to form $MgO{-}NO_x$ species, which altered the original active sites on the surface. The X-ray photoelectron spectra of two sorbents after CO_2 sorption are presented in Fig. 7d-e. The peaks at ~284.8 ev of C 1s for each sample were enhanced (Fig. 7d), confirming the CO_2 sorption process. It is also worth noting that the high-resolution spectrum of O 1s for nitrate- or nitrite-coated MgO (Fig. 7e) shows only one peak assigned to carbonate species at ~531.8 ev with an enhanced intensity, while the peak at 528.5 ev belonging to hydroxyl groups disappeared, indicating that all hydroxyl groups reacted with CO_2 to form carbonate species. As indicated by the XPS analysis, the active sites covered by atmospheric CO_2 for $MgO/0.2NaNO_2$ were larger than those for $MgO/0.2NaNO_3$. During the preheating process before the CO_2 sorption tests, these active sites were easily recovered and were responsible for generating more carbonate species. Thus, the induction time for $MgO/0.2NaNO_2$ was sharply reduced (less than 1 min). Moreover, as supported by the above characterizations, the presence of more hydroxide sites and carbonate species on the surface of MgO is likely responsible for the superior performance of $MgO/0.2NaNO_2$.

The cyclic performance of the nitrate- or nitrite-coated MgO sorbents was further examined by means of a test with 10 sorption/desorption cycles. As shown in Fig. 8, the initial CO_2 uptake of $MgO/0.2NaNO_2$ reached 0.55 g/g, slightly higher than that of

$MgO/0.2NaNO_3$. After 10 cycles, this value decreased to 0.29 g/g, which is still twice that for $MgO/0.2NaNO_3$, confirming that the regeneration capability of $MgO/0.2NaNO_2$ is better than that of $MgO/0.2NaNO_3$. Here, the reaction rate of $MgO/0.2NaNO_2$ is faster than that of $MgO/0.2NaNO_3$ over 10 cycles. To explore its cyclic performance, the decomposition behavior of $MgCO_3$ was examined with and without alkali nitrates/nitrites. As shown in Fig. 9, coating with alkali nitrates/nitrites facilitated CO_2 desorption from $MgCO_3$. In particular, the decomposition temperature was even lower in the presence of $NaNO_2$, causing less sintering of the cycled $MgO/0.2NaNO_2$, thus, responsible for its better cyclic performance.

3.3 Kinetic analysis

According to the isothermal results, the CO_2 sorption during the induction step appears to be negligible. Thus, different isothermal data excluding the induction step at 240-300 °C were fitted with the following model to analyze the influence of $NaNO_3$ and $NaNO_2$ addition on the sorption kinetics [48]:

$$y = A\exp(-k_1 t) + B\exp(-k_2 t) + C \qquad (1)$$

where y represents the CO_2 sorption capacity; t represents the time; A, B and C are the pre-exponential factors; and k_1 and k_2 represent the exponential constants indicating the CO_2 surface chemisorption directly on the MgO particles, and the product layer diffusion process, respectively.

As shown in Fig. 10, the CO_2 sorption behavior on $MgO/0.2NaNO_3$ is well-described by the double-exponential model. The exponential constants calculated from this model are shown in Table 2. The k_1 values at different temperatures for

$MgO/0.2NaNO_3$ and $MgO/0.2NaNO_2$ are far higher than the corresponding k_2 values, implying that the product layer diffusion became the main restrictive factor during the entire sorption process. Moreover, the values of k_1 for $MgO/0.2NaNO_2$ were far higher than those for $MgO/0.2NaNO_3$, meaning that $NaNO_2$ acts as a more efficient promoter for the surface chemisorption stage.

Next, the Arrhenius model was used to estimate the activation energies involved in different stages of the two samples:

$$k = k_0 \exp^{(-E/RT)} \qquad (2)$$

where k is the reaction rate constant, k_0 is the pre-exponential factor, E is the activation energy, R is the gas constant, and T is the absolute temperature.

Fig. 11 shows that the plots of ln k versus $1/T$ show good curve fits. The kinetic analysis dependence on temperature range showed that $MgO/0.2NaNO_3$ and $MgO/0.2NaNO_2$ presented completely different behaviors. A large activation energy value usually indicates a strong dependence on temperature. For $MgO/0.2NaNO_3$, the activation energy values for the surface chemisorption approached those for the product layer diffusion, indicating that both steps have similar dependence on temperature. Moreover, the larger activation energy values as compared with those in $MgO/0.2NaNO_2$, suggested that the surface chemisorption and the product layer diffusion are both strongly dependent on temperature. On the other hand, for $MgO/0.2NaNO_2$, the activation energy value for the surface chemisorption was only ~2.0 kJ/mol, which is several orders of magnitude smaller than that for the product layer diffusion. This observation suggested that surface chemisorption was not

dependent on temperature in this case. Compared with $NaNO_3$, $NaNO_2$ produced a higher concentration of oxide ions (O^{2-}) in the molten state, thus generating more CO_3^{2-} with Mg^{2+} derived from the dissolved MgO to form the $MgCO_3$ crystals on the surface [26]. As supported by FTIR and XPS results, more hydroxide sites on the surface were also generated for $MgO/0.2NaNO_2$, providing more active sites for surface chemisorption. This hypothesis was also verified here by means of FTIR analysis (Fig. 6b) as follows.

After CO_2 sorption of $MgO/0.2NaNO_2$, the peaks corresponding to O-H stretching vibrations for various types of hydroxyl groups completely disappeared and three large peaks at 1355, 886, and 749 cm^{-1} attributed to different types of carbonate ions (CO_3^{2-}) [44] were observed, indicating that the hydroxide sites on the surface were replaced by carbonate ions after reaction with CO_2. Additionally, the presence of more carbonate species on the surface for $MgO/0.2NaNO_2$ facilitated the conversion of carbonate species to CO_3^{2-} [41]. All these factors favored the surface chemisorption process, reducing the energy required for the reaction. However, as this process progressed, the $MgCO_3$ layer grew thicker, greatly increasing the counter-current diffusion of inward CO_3^{2-} and outward O^{2-}, which then serve as barriers to further reaction with the remaining MgO [31].

4. Conclusions

Two types of alkali metal nitrate-/nitrite-promoted MgO sorbents showed markedly improved CO_2 capture performance compared with pure MgO. In particular, $NaNO_2$-promoted MgO demonstrated a much shorter induction time, faster sorption

rate, higher uptake capacity and better stability over a wider temperature range, indicating that $NaNO_2$ serves as an efficient additive. $NaNO_2$-promoted MgO also presented bimodal sorption characteristics which has not been previously reported, which appear to result from the presence of double promoters (a mixture of $NaNO_2$ and $NaNO_3$). In addition, different amounts of $NaNO_2$ significantly affected the sorption characteristics of the promoted MgO sorbents. The optimal proportion of $NaNO_2$ here is 20 wt%.

Characterization results revealed that part of the nitrite is oxidized to nitrate during the preparation process. These double promoters were coated on the MgO surface due to an increased crystallite size of MgO, and resulted in relatively sintered and rough morphologies, and reduced surface area/pore volume. As a consequence, the $NaNO_2$ promoted sorbent had larger concentrations of hydroxide sites and carbonate species on the surface, which was associated with more active sites for CO_2 capture.

As experimental work was done over a range of temperatures, this permitted for the first time, a kinetics analysis which showed that a double exponential model fits well for CO_2 sorption behavior of $NaNO_2$-promoted sorbent, suggesting that a double sorption process including surface chemisorption and product layer diffusion occurs. Here, the activation energy for the surface chemisorption was only ~2.0 kJ/mol, which was several orders of magnitude smaller than that for the product layer diffusion. Due to the presence of more abundant active hydroxide sites and carbonate species on the surface, the surface chemisorption process was greatly facilitated. It is, therefore,

evident that the entire sorption process dependence on temperature was primarily limited by the diffusion process.

Supplementary material

The DTG curves of different sorbents. (a) $NaNO_2$ and $NaNO_3$ co-doped MgO with molar ratio of $NaNO_2$ to $NaNO_3$ at 0.09:0.11; (b) MgO/$NaNO_3$ with different amounts of $NaNO_3$; (c) $NaNO_3$ and $NaCO_3$ co-doped MgO with different molar ratios of $NaCO_3$ (Fig. S1), SEM images of (a) MgO/0.2$NaNO_3$ and (b) MgO/0.2$NaNO_2$ (Fig. S2) and FTIR spectra of MgO/0.2$NaNO_3$ and MgO/0.2$NaNO_2$ normalized by the absorbance at 1384 cm^{-1} (NO^{3-}) (Fig. S3).

Acknowledgement

This work was supported by financial support from the Fundamental Research Funds for the Central Universities, China (2015XKMS054).

References

[1] S. Brune, S.E. Williams, R.D. Müller, Potential links between continental rifting, CO_2 degassing and climate change through time, Nat. Geosci. 10 (2017) 941-946.

[2] IEA, CO_2 Emissions from Fuel Combustion 2018, 2018.

[3] M. Bui, C.S. Adjiman, A. Bardow, E.J. Anthony, A. Boston, S. Brown, P.S. Fennell, S. Fuss, A. Galindo, L.A. Hackett, J.P. Hallett, H.J. Herzog, G. Jackson, J. Kemper, S. Krevor, G.C. Maitland, M. Matuszewski, I.S. Metcalfe, C. Petit, G. Puxty, J. Reimer, D.M. Reiner, E.S. Rubin, S.A. Scott, N. Shah, B. Smit, J.P.M. Trusler, P. Webley, J. Wilcox, N. Mac Dowell, Carbon capture and storage (CCS): the way forward, Energy Environ. Sci. 11 (2018) 1062-1176.

[4] A. Perejon, L.M. Romeo, Y. Lara, P. Lisbona, A. Martinez, J. Manuel Valverde, The Calcium-Looping technology for CO_2 capture: On the important roles of energy integration and sorbent behavior, Appl. Energy 162 (2016) 787-807.

[5] D.P. Hanak, E.J. Anthony, V. Manovic, A review of developments in pilot-plant testing and modelling of calcium looping process for CO_2 capture from power generation systems, Energy Environ. Sci. 8 (2015) 2199-2249.

[6] M.A. Nemitallah, M.A. Habib, H.M. Badr, S.A. Said, A. Jamal, R. Ben-Mansour, E.M.A. Mokheimer, K. Mezghani, Oxy-fuel combustion technology: current status, applications, and trends, Int. J. Energy Res. 41 (2017) 1670-1708.

[7] A. Samanta, A. Zhao, G.K.H. Shimizu, P. Sarkar, R. Gupta, Post-Combustion CO_2 Capture Using Solid Sorbents: A Review, Ind. Eng. Chem. Res. 51 (2012) 1438-1463.

[8] M. Asif, M. Suleman, I. Haq, S.A. Jamal, Post-combustion CO_2 capture with chemical absorption

and hybrid system: current status and challenges, Greenh. Gases 8 (2018) 998-1031.

[9] C.A. Scholes, K.H. Smith, S.E. Kentish, G.W. Stevens, CO_2 capture from pre-combustion processes-Strategies for membrane gas separation, Int. J. Greenhouse Gas Control 4 (2010) 739-755.

[10] P. Linga, M.A. Clarke, A Review of Reactor Designs and Materials Employed for Increasing the Rate of Gas Hydrate Formation, Energy Fuels 31 (2017) 1-13.

[11] M.S. Yancheshmeh, H.R. Radfarnia, M.C. Iliuta, High temperature CO_2 sorbents and their application for hydrogen production by sorption enhanced steam reforming process, Chem. Eng. J. 283 (2016) 420-444.

[12] G. Ji, J.G. Yao, P.T. Clough, J.C.D. da Costa, E.J. Anthony, P.S. Fennell, W. Wang, M. Zhao, Enhanced hydrogen production from thermochemical processes, Energy Environ. Sci. 11 (2018) 2647-2672.

[13] S.I. Garces-Polo, J. Villarroel-Rocha, K. Sapag, S.A. Korili, A. Gil, Adsorption of CO_2 on mixed oxides derived from hydrotalcites at several temperatures and high pressures, Chem. Eng. J. 332 (2018) 24-32.

[14] L.K.G. Bhatta, S. Subramanyam, M.D. Chengala, S. Olivera, K. Venkatesh, Progress in hydrotalcite like compounds and metal-based oxides for CO_2 capture: a review, J. Clean. Prod. 103 (2015) 171-196.

[15] E. Abbasi, A. Hassanzadeh, S. Zarghami, H. Arastoopour, J. Abbasian, Regenerable MgO-based sorbent for high temperature CO_2 removal from syngas: 3. CO_2 capture and sorbent enhanced water gas shift reaction, Fuel 137 (2014) 260-268.

[16] K. Kim, J.W. Han, K.S. Lee, W.B. Lee, Promoting alkali and alkaline-earth metals on MgO for enhancing CO_2 capture by first-principles calculations, PCCP 16 (2014) 24818-24823.

[17] A. Hanif, S. Dasgupta, A. Nanoti, Facile Synthesis of High-Surface-Area Mesoporous MgO with Excellent High-Temperature CO_2 Adsorption Potential, Ind. Eng. Chem. Res. 55 (2016) 8070-8078.

[18] S. Shahkarami, A.K. Dalai, J. Soltan, Enhanced CO_2 Adsorption Using MgO-Impregnated Activated Carbon: Impact of Preparation Techniques, Ind. Eng. Chem. Res. 55 (2016) 5955-5964.

[19] C. Hai, Y. Zhou, Y. Du, Y. Sun, J. Zeng, Y. Shen, X. Ren, X. Li, L. Zhang, O. Dong, Synthesis of MgO nanocrystals with abundant surface defects via a carbonization method employing CO_2 gas as starting material, Mater. Res. Bull. 85 (2017) 181-187.

[20] W. Gao, T. Zhou, Y. Gao, B. Louis, D. O'Hare, Q. Wang, Molten salts-modified MgO-based adsorbents for intermediate-temperature CO2 capture: A review, J. Ener. Chem. 26 (2017) 830-838.

[21] B.W. Hwang, J.H. Lim, H.J. Chae, H.-J. Ryu, D. Lee, J.B. Lee, H. Kim, S.C. Lee, J.C. Kim, CO_2 capture and regeneration properties of MgO-based sorbents promoted with alkali metal nitrates at high pressure for the sorption enhanced water gas shift process, Process. Saf. Environ 116 (2018) 219-227.

[22] S. Zarghami, A. Hassanzadeh, H. Arastoopour, J. Abbasian, Effect of Steam on the Reactivity of MgO-Based Sorbents in Precombustion CO_2 Capture Processes, Ind. Eng. Chem. Res. 54 (2015) 8860-8866.

[23] X. Yang, L. Zhao, Y. Xiao, Effect of $NaNO_3$ on MgO-$CaCO_3$ Absorbent for CO_2 Capture at Warm Temperature, Energy Fuels 27 (2013) 7645-7653.

[24] A.K. Prashar, H. Seo, W.C. Choi, N.Y. Kang, S. Park, K. Kim, D.Y. Min, H.M. Kim, Y.K. Park, Factors Affecting the Rate of CO_2 Absorption after Partial Desorption in $NaNO_3$-Promoted MgO, Energy Fuels 30 (2016) 3298-3305.

[25] Y. Hu, X. Liu, Z. Zhou, W. Liu, M. Xu, Pelletization of MgO-based sorbents for intermediate temperature CO_2 capture, Fuel 187 (2017) 328-337.

[26] S.I. Jo, Y.I. An, K.Y. Kim, S.Y. Choi, J.S. Kwak, K.R. Oh, Y.U. Kwon, Mechanisms of absorption and desorption of CO_2 by molten $NaNO_3$-promoted MgO, PCCP 19 (2017) 6224-6232.

[27] M.L.T. Triviño, V. Hiremath, J.G. Seo, Stabilization of $NaNO_3$-Promoted Magnesium Oxide for High-Temperature CO_2 Capture, Environ. Sci. Technol. 52 (2018) 11952-11959.

[28] S.C. Lee, S.H. Cha, Y.M. Kwon, M.G. Park, B.W. Hwang, Y.K. Park, H.M. Seo, J.C. Kim, Effects of alkali-metal carbonates and nitrates on the CO_2 sorption and regeneration of MgO-based sorbents at intermediate temperatures, Korean J. Chem. Eng. 33 (2016) 3448-3455.

[29] A.T. Vu, K. Ho, S. Jin, C.H. Lee, Double sodium salt-promoted mesoporous MgO sorbent with high CO_2 sorption capacity at intermediate temperatures under dry and wet conditions, Chem. Eng. J. 291 (2016) 161-173.

[30] S. Jin, K. Ho, C.H. Lee, Facile synthesis of hierarchically porous MgO sorbent doped with $CaCO_3$ for fast CO_2 capture in rapid intermediate temperature swing sorption, Chem. Eng. J. 334 (2018) 1605-1613.

[31] X. Zhao, G. Ji, W. Liu, X. He, E.J. Anthony, M. Zhao, Mesoporous MgO promoted with $NaNO_3$/$NaNO_2$ for rapid and high-capacity CO_2 capture at moderate temperatures, Chem. Eng. J. 332 (2018) 216-226.

[32] T. Harada, T.A. Hatton, Colloidal Nanoclusters of MgO Coated with Alkali Metal Nitrates/Nitrites for Rapid, High Capacity CO_2 Capture at Moderate Temperature, Chem. Mater. 27 (2015) 8153-8161.

[33] T. Harada, F. Simeon, E.Z. Hamad, T.A. Hatton, Alkali Metal Nitrate-Promoted High-Capacity MgO Adsorbents for Regenerable CO_2 Capture at Moderate Temperatures, Chem. Mater. 27 (2015) 1943-1949.

[34] Y. Qiao, J. Wang, Y. Zhang, W. Gao, T. Harada, L. Huang, T.A. Hatton, Q. Wang, Alkali Nitrates Molten Salt Modified Commercial MgO for Intermediate-Temperature CO_2 Capture: Optimization of the Li/Na/K Ratio, Ind. Eng. Chem. Res. 56 (2017) 1509-1517.

[35] W. Gao, T. Zhou, Y. Gao, Q. Wang, W. Lin, Study on MNO_3/NO_2 (M = Li, Na, and K)/MgO Composites for Intermediate-Temperature CO_2 Capture, Energy Fuels (2018) DOI: 10.1021/acs.energyfuels.1028b02749.

[36] L. Wang, Z. Zhou, Y. Hu, Z. Cheng, X. Fang, Nanosheet MgO-Based CO_2 Sorbent Promoted by Mixed-Alkali-Metal Nitrate and Carbonate: Performance and Mechanism, Ind. Eng. Chem. Res. 56 (2017) 5802-5812.

[37] H. Cui, Q. Zhang, Y. Hu, C. Peng, X. Fang, Z. Cheng, V.V. Galvita, Z. Zhou, Ultrafast and Stable CO_2 Capture Using Alkali Metal Salt-Promoted MgO–$CaCO_3$ Sorbents, ACS Appl. Mat. Interfaces 10 (2018) 20611-20620.

[38] G. Xiao, R. Singh, A. Chaffee, P. Webley, Advanced adsorbents based on MgO and K_2CO_3 for capture of CO_2 at elevated temperatures, Int. J. Greenhouse Gas Control 5 (2011) 634-639.

[39] T. Eom, J. Lee, K. Kim, C. Ryu, Y. Rhee, Characteristics of Spray-Dried K_2CO_3-MgO Solid Sorbent for CO_2 Capture from Power Plant Flue Gas, J. Chem. Eng. Jpn. 50 (2017) 213-220.

[40] A.-T. Vu, Y. Park, P.R. Jeon, C.-H. Lee, Mesoporous MgO sorbent promoted with KNO_3 for CO_2 capture at intermediate temperatures, Chem. Eng. J. 258 (2014) 254-264.

[41] K. Zhang, X.S. Li, W.Z. Li, A. Rohatgi, Y. Duan, P. Singh, L. Li, D.L. King, Phase Transfer-Catalyzed Fast CO_2 Absorption by MgO-Based Absorbents with High Cycling Capacity, Adv. Mater. Interfaces. 1 (2014) 1400030.

[42] H. Lee, M.L.T. Triviño, S. Hwang, S.H. Kwon, S.G. Lee, J.H. Moon, J. Yoo, J.G. Seo, In Situ Observation of Carbon Dioxide Capture on Pseudo-Liquid Eutectic Mixture-Promoted Magnesium

Oxide, ACS Appl. Mat. Interfaces 10 (2018) 2414-2422.

[43] K. Zhang, X.S. Li, H. Chen, P. Singh, D.L. King, Molten Salt Promoting Effect in Double Salt CO_2 Absorbents, J. Phys. Chem. C 120 (2016).

[44] R. Philipp, K. Fujimoto, FTIR spectroscopic study of CO_2 adsorption/desorption on MgO/CaO catalysts, J. Phys. Chem. 96 (1992) 9035-9038.

[45] S.-W. Bian, J. Baltrusaitis, P. Galhotra, V.H. Grassian, A template-free, thermal decomposition method to synthesize mesoporous MgO with a nanocrystalline framework and its application in carbon dioxide adsorption, J. Mater. Chem. 20 (2010) 8705-8710.

[46] T.W. Elkins, S.J. Roberts, H.E. Hagelin-Weaver, Effects of alkali and alkaline-earth metal dopants on magnesium oxide supported rare-earth oxide catalysts in the oxidative coupling of methane, Applied Catalysis a-General 528 (2016) 175-190.

[47] D.K. Aswal, K.P. Muthe, S. Tawde, S. Chodhury, N. Bagkar, A. Singh, S.K. Gupta, J.V. Yakhmi, XPS and AFM investigations of annealing induced surface modifications of MgO single crystals, J. Cryst. Growth 236 (2002) 661-666.

[48] M.J. Venegas, E. Fregoso-Israel, R. Escamilla, H. Pfeiffer, Kinetic and Reaction Mechanism of CO_2 Sorption on Li_4SiO_4:Study of the Particle Size Effect, Ind. Eng. Chem. Res. 46 (2007) 2407-2412.

Figure captions:

Fig. 1. CO_2 uptake by alkali metal nitrate-/nitrite-coated MgO samples in 100% CO_2 atmosphere. (a) Dynamic CO_2 uptake variations of MgO coated with 20 wt% $NaNO_3$ and different ratios of $NaNO_2$ between 100-600°C; (b) Derivative thermogravimetry curves of the sorbents corresponding to Fig 1a.

Fig. 2. Isothermal sorption curves of MgO coated with nitrate/nitrite at different temperatures. (a) the isotherms of MgO/0.2$NaNO_3$ at different temperatures; (b) the isotherms of MgO/0.2$NaNO_2$ at different temperatures; (c) the isotherms of MgO/0.2$NaNO_3$ between 0-5 minutes at different temperatures.

Fig. 3. XRD patterns of the different sorbents.

Fig. 4. SEM images of samples. (a) uncoated MgO (10 μm); (b) uncoated MgO (1μm); (c) MgO/0.2$NaNO_3$ (1 μm); and (d) MgO/0.2$NaNO_2$ (1 μm).

Fig. 5. (a) N_2 adsorption-desorption isotherms of MgO, MgO/0.2$NaNO_3$ and MgO/0.2$NaNO_2$; (b) BJH pore size distribution of different sorbents.

Fig. 6. FTIR spectra of the samples. (a) fresh sorbents; (b) after sorption.

Fig. 7. X-ray photoelectron spectra of the three sorbents. (a) survey scanned spectra of fresh sorbent; (b) the high-resolution spectra of Na 1s of fresh sorbent; (c) the high-resolution spectra of O 1s of fresh sorbent; (d) survey scanned spectra of sorbent after sorption; (e) the high-resolution spectra of O 1s of sorbent after sorption.

Fig. 8. CO_2 uptake over repeated cycles of CO_2 sorption in 100% CO_2 and desorption in 100% N_2 for MgO/0.2$NaNO_3$ and MgO/0.2$NaNO_2$.

Fig. 9. Decomposition behavior of $MgCO_3$, $MgCO_3/0.2NaNO_3$ and $MgCO_3/0.2NaNO_2$ through thermogravimetric analysis

Fig. 10. Comparison of CO_2 uptake of $MgO/0.2NaNO_3$ (solid line) plotted according to the expected kinetic models (dotted line).

Fig. 11. Kinetic analysis of $MgO/0.2NaNO_3$ and $MgO/0.2NaNO_2$.

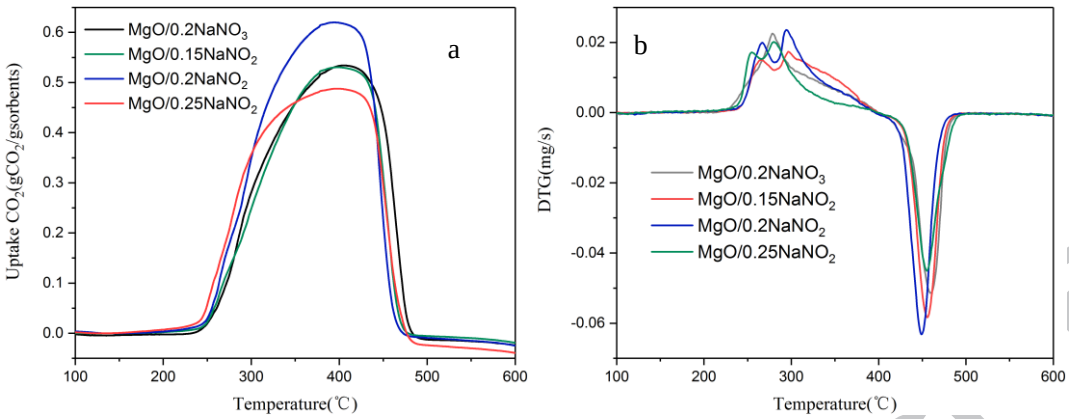

Fig. 1.

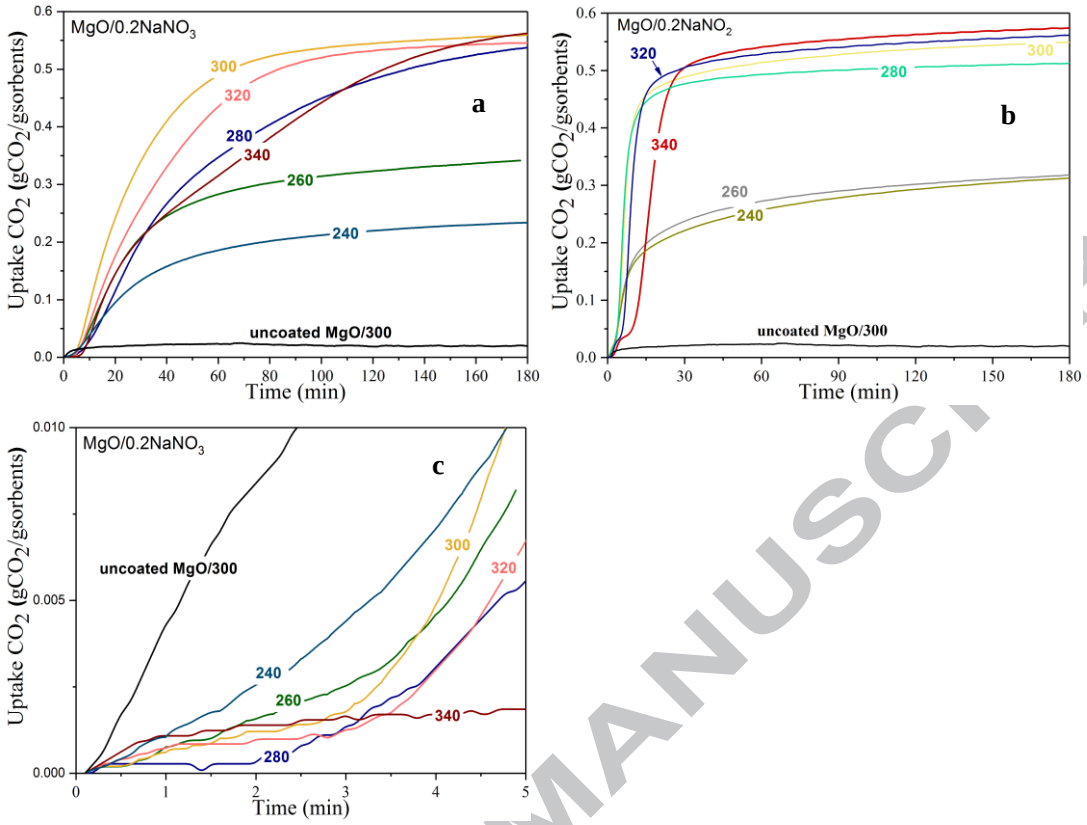

Fig. 2.

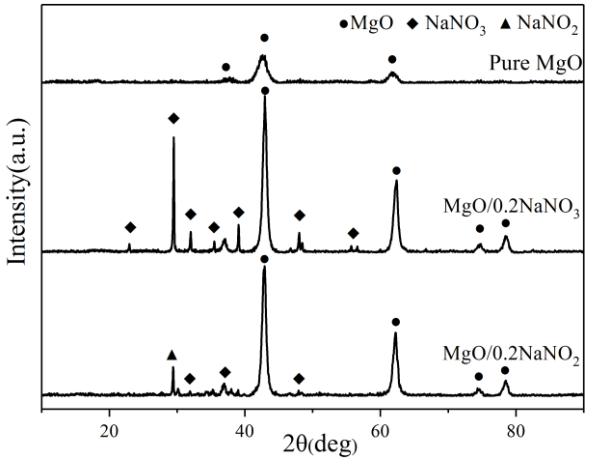

Fig. 3.

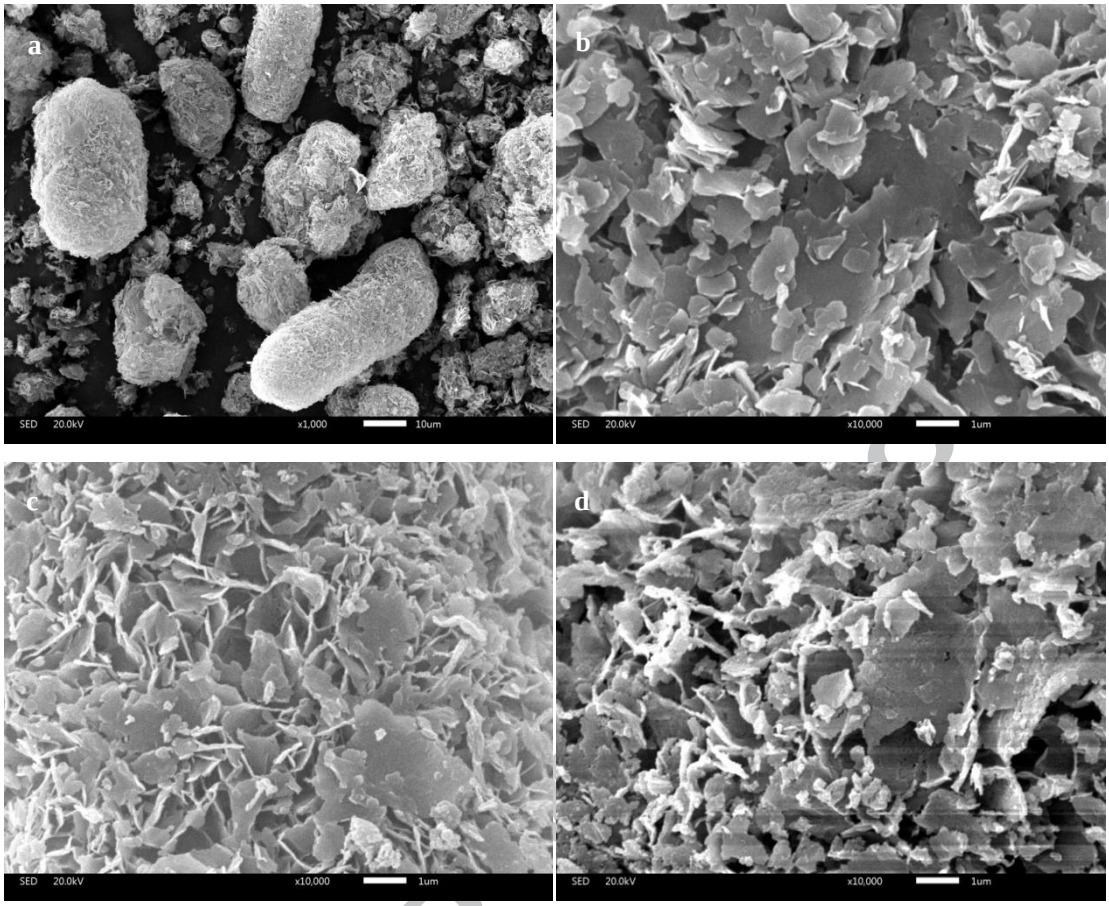

Fig. 4.

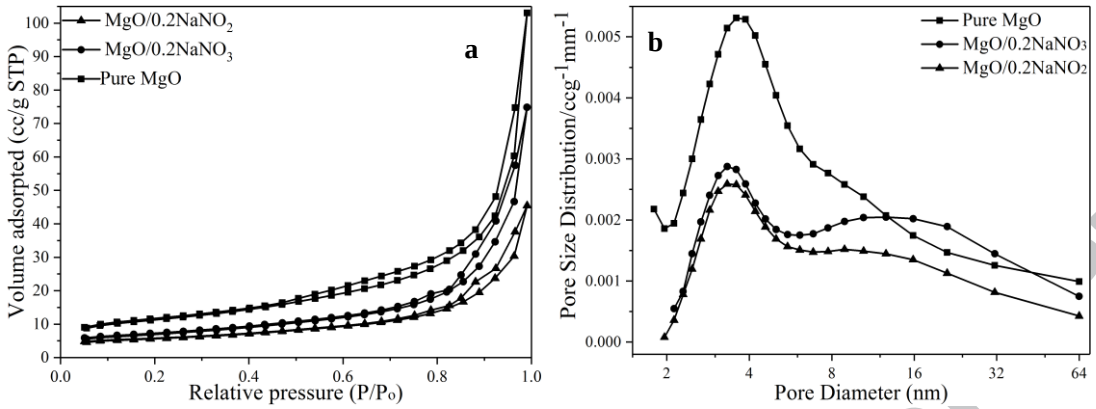

Fig. 5.

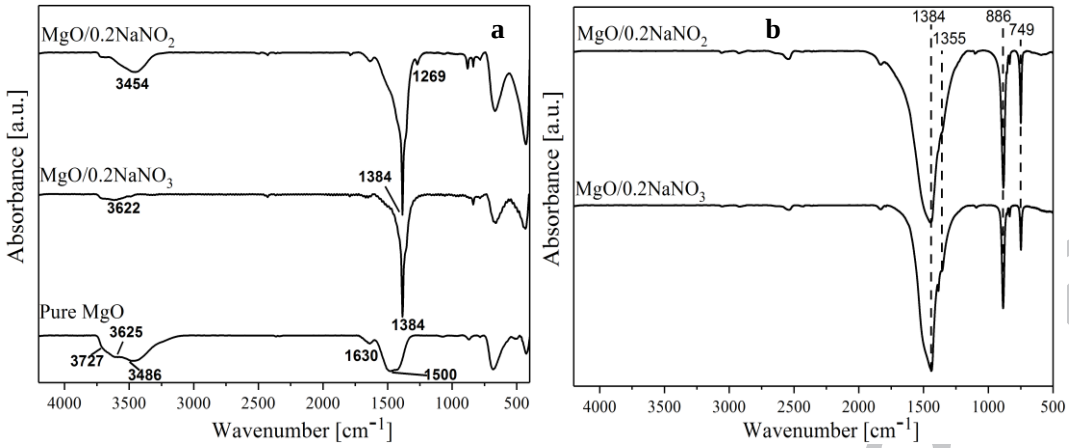

Fig. 6.

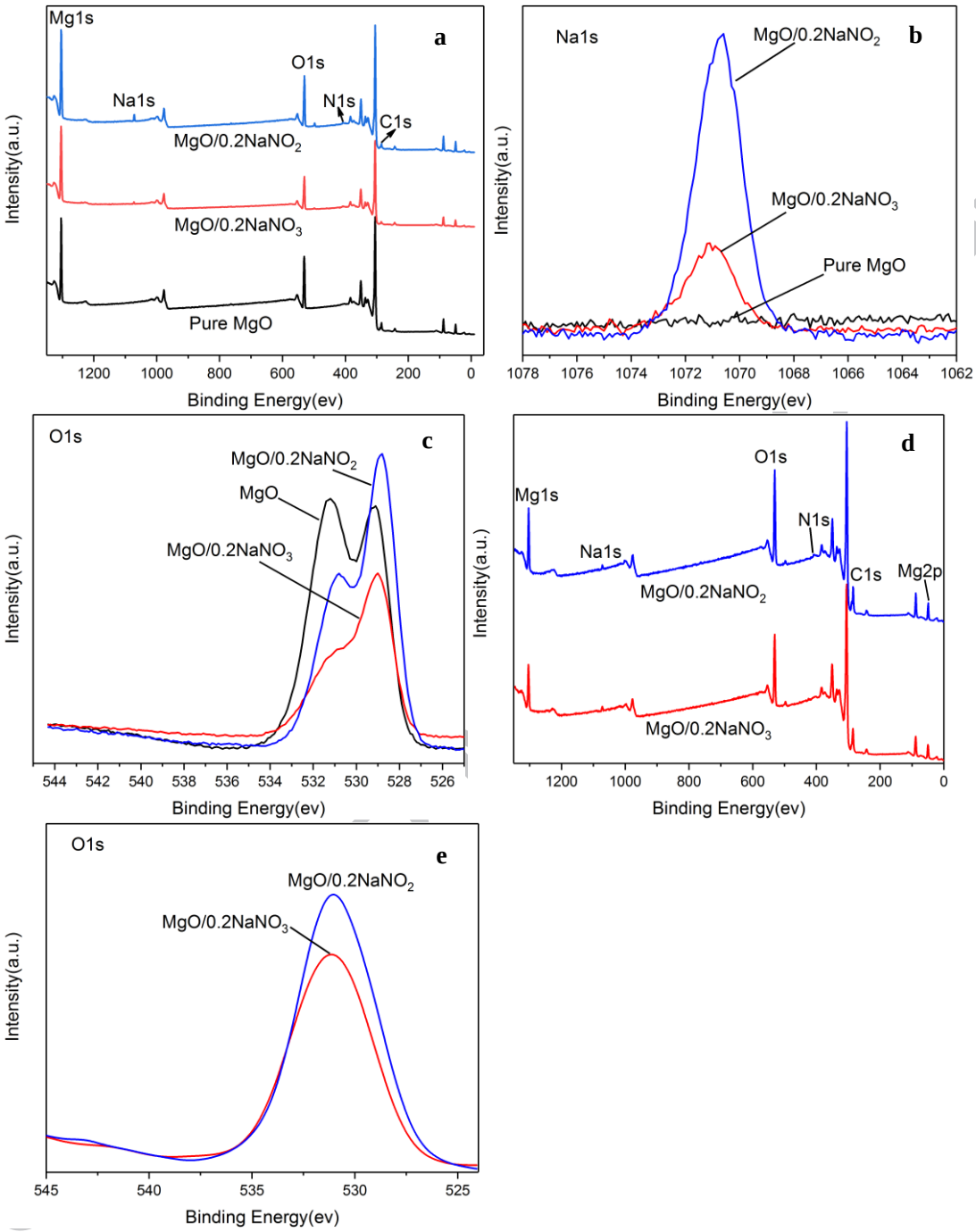

Fig. 7.

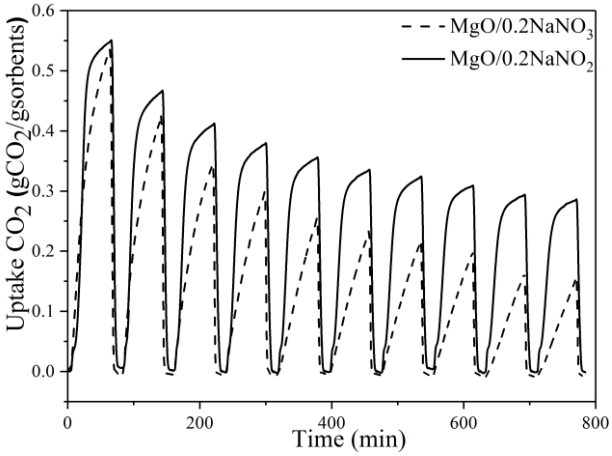

Fig. 8.

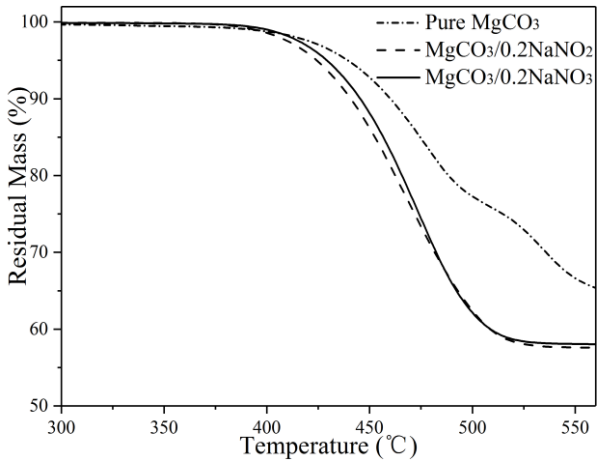

Fig. 9.

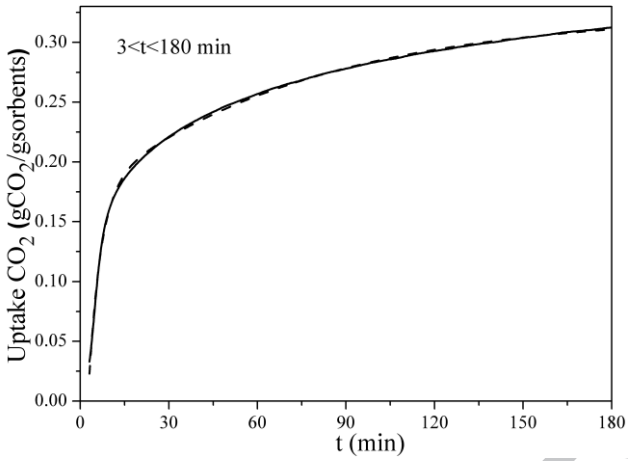

Fig. 10.

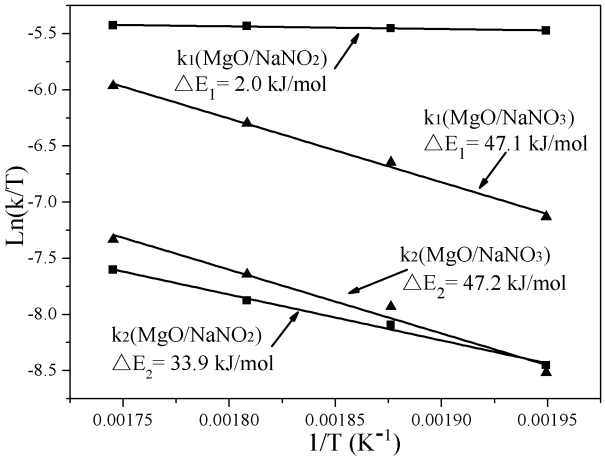

Fig. 11.

Table 1 Properties of different prepared sorbents.

Samples	Surface area (m^2/g)	Pore volume (cm^3/g)	Pore size (nm)	Crystalline size (nm)
Pure MgO	39.23	0.16	16.2	8.0
$MgO/0.2NaNO_3$	24.21	0.12	19.1	14.3
$MgO/0.2NaNO_2$	19.24	0.07	14.6	13.7

Table 2. Kinetic parameters obtained from the isotherms of $MgO/0.2NaNO_3$ and $MgO/0.2NaNO_2$ sorbents.

T [°C]	$MgO/0.2NaNO_3$			$MgO/0.2NaNO_2$		
	k_1	k_2	R	k_1	k_2	R
240	8.00×10^{-4}	2.00×10^{-4}	0.999	4.20×10^{-3}	2.13×10^{-4}	0.999
260	1.30×10^{-3}	3.60×10^{-4}	0.997	4.28×10^{-3}	3.06×10^{-4}	0.999
280	1.84×10^{-3}	4.80×10^{-4}	0.999	4.37×10^{-3}	3.80×10^{-4}	0.996
300	2.57×10^{-3}	6.54×10^{-4}	0.999	4.40×10^{-3}	5.00×10^{-4}	0.992

Highlights:

A $NaNO_2$-promoted MgO for CO_2 capture was prepared and characterized.

Doped $NaNO_2$ induced significant quantities of hydroxide sites and carbonate species.

These desirable features facilitated surface chemisorption processes.

The surface chemisorption process was not dependent on temperature.